Available online at www.sciencedirect.com
ScienceDirect
Materials Letters 61 (2007) 3500–3503
materials letters
www.elsevier.com/locate/matlet

Orientation and growth behavior of $CaHfO_3$ thin films on non-oxide substrates

Y.W. Kwon [a], D.P. Norton [a,*], John D. Budai [b]

[a] University of Florida, Department of Materials Science and Engineering, 106 Rhines Hall, Gainesville, FL 32611, USA
[b] Oak Ridge National Laboratory, Materials Science and Technology Division, Oak Ridge, TN 37831-6030, USA

Received 22 July 2006; accepted 21 November 2006
Available online 8 December 2006

Abstract

The growth behavior of $CaHfO_3$ on (001) Ni and Ge substrates was examined. $CaHfO_3$ is a perovskite insulator that is suitable for applications as a buffer layer or gate dielectric. The tendency for $CaHfO_3$ growth on both (001) Ni and (001) Ge substrates is to orient with the $CaHfO_3$ (200)+(121) planes parallel to the surface, which corresponds to the (110) orientation in the pseudo-cubic geometry. This differs from that of $CaHfO_3$ on perovskites, such as (001) $LaAlO_3$, where a pseudo-cube-on-cube orientation is observed.
© 2006 Elsevier B.V. All rights reserved.

In recent years, significant interest has emerged in the epitaxial growth of perovskite oxides on various substrates, including non-oxide substrate materials [1–5]. Perovskites exhibit an extraordinary range of properties, from superconducting metals to ferroelectric insulators. Significant attention has been given to the growth of titanate, niobate, and manganite thin films due to their ferroelectric and magnetic characteristics. There is also interest in the use of wide gap dielectric perovskites as gate dielectrics and buffer layers on non-oxide substrate materials. Epitaxial growth of perovskites as alternative gate dielectrics for silicon or germanium-based metal-oxide-semiconductor field-effect transistor technology has been studied for a number of materials [1,6–8]. Novel epitaxial gate dielectric structures have also been explored for electric field gating of oxide semiconductor transport [9]. As a buffer layer, the growth of epitaxial oxides on metallic substrates is a prerequisite for developing high temperature superconducting coated conductors based on epitaxial superconducting oxides on biaxially textured metal tapes [10,11].

One class of perovskite dielectric that has attractive bulk properties but has received limited attention in thin film research is the hafnates [12,13]. Interest in hafnate perovskites as buffer layer materials stems from their limited reactivity with other materials. For example, experiments in which mixtures of $YBa_2Cu_3O_{7-x}$ and $BaHfO_3$ were heated to high temperatures indicate that these compounds do not react significantly up to 1000 °C [14]. These characteristics make hafnate perovskites attractive as buffer layers for oxide growth on semiconductor and metal substrates. Hafnates also exhibit luminescence when doped with rare earth elements, making them potential scintillating materials [15,16]. Luminescence is observed in $MHfO_3$:Ce (M=Ba, Sr, or Ca) from Ce^{3+} *5d* to *4f* transitions when subjected to ultraviolet light excitation [17]. In addition, their large bandgap makes them of interest as a gate dielectric for wide gap semiconductors. Field-effect transistor structures have been fabricated in which amorphous $CaHfO_3$ serves as the gate dielectric for a semiconducting $SrTiO_3$ channel [17]. In this paper, we discuss the growth behavior of $CaHfO_3$ films on non-oxide substrate materials, namely Ge and Ni, and compare it to the growth of $CaHfO_3$ on single crystal $LaAlO_3$.

1. Experimental procedure

Pulsed laser deposition was used to synthesize the $CaHfO_3$ thin films using an excimer KrF laser with a wavelength of 248 nm. The laser fluence was approximately ~3 J/cm^2 and repetition rate used was 5 Hz. The metal substrates used in this study were biaxially textured Ni (001) tapes prepared by thermo-mechanical processing of pure nickel [10,11]. The Ni substrate has a (001) biaxial texture with in-plane mosaic of ~13° and out-of-plane mosaic of ~9°. The Ni substrates were

* Corresponding author.
E-mail address: dnort@mse.ufl.edu (D.P. Norton).

0167-577X/$ - see front matter © 2006 Elsevier B.V. All rights reserved.
doi:10.1016/j.matlet.2006.11.092

cleaned with trichloroethylene, acetone, and methanol for 5 min. They were blown dry with nitrogen and mounted on a substrate heater using silver paint. No additional steps were employed to remove any surface layers prior to loading into the deposition chamber. The cleaning procedure for the $LaAlO_3$ substrates was identical. For deposition on Ge (100), the substrates were cleaned in a 1:10 HF:H_2O solution for 30 s, rinsed in deionized water for 60 s, ultrasonically cleaned with trichloroethylene, acetone, and methanol for 5 min and dried in N_2 to yield a hydrogen-terminated surface. The substrates were then immediately loaded into the vacuum chamber. Upon loading the substrates, the chamber was pumped to a base pressure of $\sim 2\times10^{-6}$ Torr. Approximately 100 nm-thick films were grown at temperatures ranging from 600 to 850 °C. Crystal structure and orientation was investigated using X-ray diffraction (XRD) with Cu Kα radiation (0.15405 nm wavelength).

2. Results and discussion

Initial experiments focused on $CaHfO_3$ thin films deposited on $LaAlO_3$(100) single crystal substrates. $LaAlO_3$ has a pseudo-cubic lattice parameter of 3.788 Å, providing a 5.1% lattice mismatch to the pseudo-cubic lattice parameter of 3.993 Å for $CaHfO_3$. $CaHfO_3$ has an orthorhombic crystal structure at room temperature with *a*-, *b*-, *c*-axis lattice constants of 5.719 Å, 7.982 Å and 5.577 Å respectively. The refractive index of $CaHfO_3$ was measured to be $\langle n\rangle=2.00$ at a wavelength of 500 nm. $CaHfO_3$ has a dielectric constant of 13 [18]. Its thermal expansion coefficient is $3.6\times10^{i©6}$/°C for the temperature range 100–600 °C. Fig. 1 shows that the XRD patterns for $CaHfO_3$ films grown at temperatures ranging from 500 to 750 °C in an ambient of oxygen partial pressure of 1 mTorr. Diffraction peaks from the $CaHfO_3$ are observed for growth temperatures at or above 650 °C, which indicates crystallization. The observed $CaHfO_3$ peaks correspond to the (101), (202), and (303) orthorhombic reflections, which are equivalent to the pseudo-cubic {00l} peaks. This is consistent with cube-on-cube heteroepitaxy of $CaHfO_3$ on $LaAlO_3$. The *c*-axis lattice parameter of the $CaHfO_3$ film slightly contracted as the growth temperature was increased, with a perpendicular *d*-spacing of 3.9967 Å for films grown at 650 °C and 3.9891 Å for the film grown at 750 °C. Fig. 2 shows the diffraction data as a function of oxygen partial pressure for a growth temperature of 750 °C. Note that, as the growth pressure is increased, diffraction peaks corresponding to HfO_2 (220) emerge. The *c*-axis perpendicular *d*-spacing shifts higher with higher oxygen pressure. The *d*-spacing was 3.9796 Å for a growth pressure of 10^{-4} Torr and 3.9872 Å for 50 mTorr.

Based on the growth behavior of $CaHfO_3$ on $LaAlO_3$, the growth of $CaHfO_3$ on the biaxially textured Ni substrates was examined. The epitaxial growth of oxide films on biaxially textured metal tape is one approach to achieve superconducting wires for high field, high temperature applications [10,11]. This structure, known as rolling assisted biaxially textured substrate (RABiTS), starts with metal tapes produced by thermo-mechanical texturing. The process consists of depositing buffer layers for subsequent high temperature superconducting

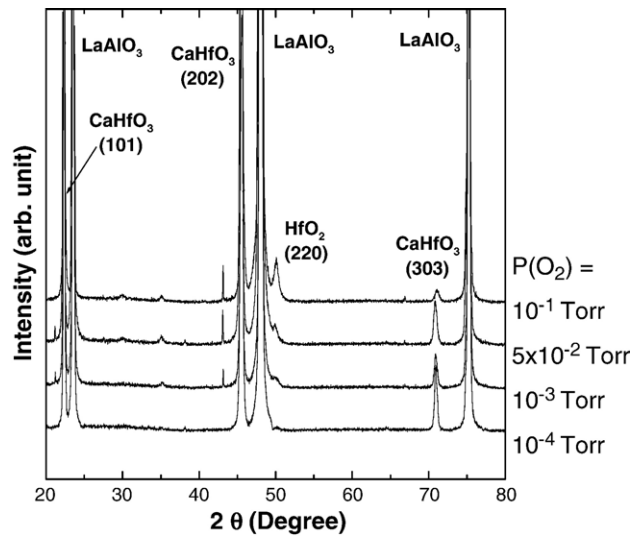

Fig. 2. X-ray diffraction scans of $CaHfO_3$ films on $LaAlO_3$ grown at 750 °C as a function of oxygen partial pressure from 10^{-4} to 10^{-1} Torr.

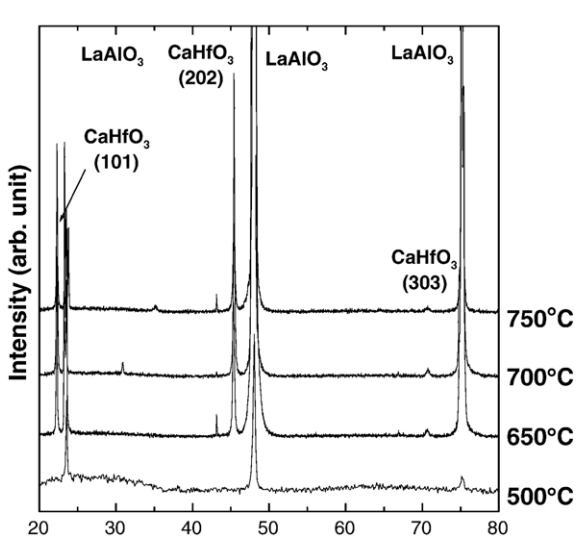

Fig. 1. X-ray diffraction scans of $CaHfO_3$ films on $LaAlO_3$ grown at 100 mTorr as a function of growth temperature from 500 to 750 °C.

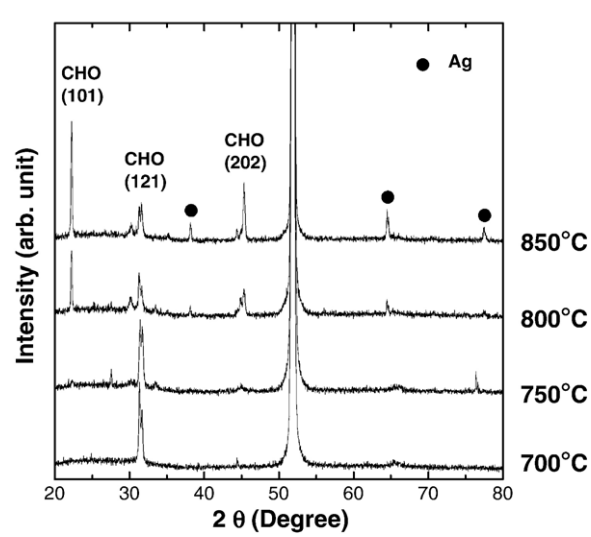

Fig. 3. X-ray diffraction scans of $CaHfO_3$ films grown on (001) biaxially textured Ni at temperature ranging from 700 to 850 °C in vacuum with a repetition rate of 2 Hz.

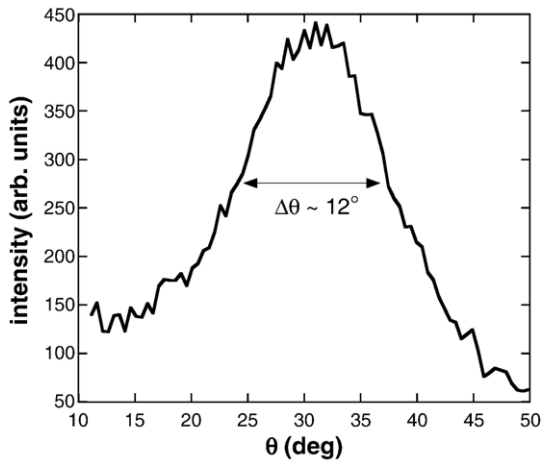

Fig. 4. Rocking curve for $CaHfO_3$ film grown on biaxially textured Ni.

film growth on the biaxially textured flexible metal substrates. Nickel and related alloys are the most commonly used starting template in the RABiTS process. Fig. 3 shows the XRD patterns of $CaHfO_3$ thin films grown in vacuum ambient at the temperature range of 700 to 850 °C. The orientation of the film was dependent on growth temperature, with the orthorhombic $CaHfO_3$ (200)+(121) (pseudo-cubic (110)) orientation observed at lower temperature, the $CaHfO_3$ (101) (pseudo-cubic (001)) orientation emerging at higher temperature. Under no conditions was the $CaHfO_3$ oriented solely as pseudo-cubic (001) as seen on $LaAlO_3$. For the film grown at 700 °C, a low resolution θ–2θ scan along the surface normal shows mostly $CaHfO_3$ (200)+(121) and $CaHfO_3$ (400)+(242), with a small amount of $CaHfO_3$ (101). A high resolution scan through the $CaHfO_3$ (200)+(121) along the surface normal shows two peaks (d=2.853 Å, 2.826 Å). These d-spacings appear closest to bulk (200)-perp and (121)-perp orientation, i.e. pseudo-cubic (110)-perpendicular $CaHfO_3$. A θ-scan through the $CaHfO_3$ (400)+(242), shown in Fig. 4, has a $\Delta\theta$=12°. Note that the Ni (002) peak width is slightly narrower. ϕ-scans show in-plane alignment that is a bit unexpected. ϕ-scans through the $CaHfO_3$ (202), shown in Fig. 5, show narrow peaks at ±90°, broader peaks at 0° and 180°, and some intensity at all orientations. Out-of-plane, the specific orientation of the $CaHfO_3$ relative to the cubic Ni corresponds to the

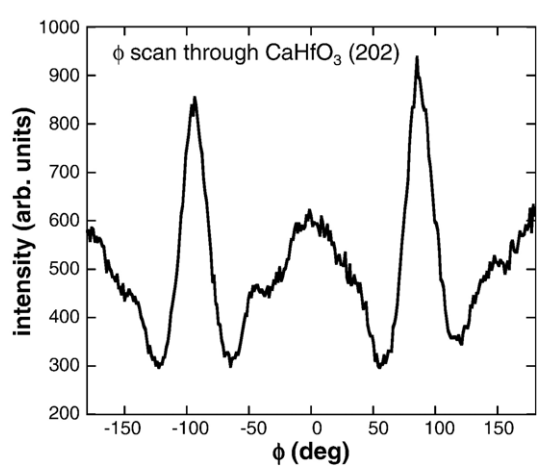

Fig. 5. ϕ-scan through the $CaHfO_3$ (202) for a film grown on biaxially textured Ni. χ=45° for this scan.

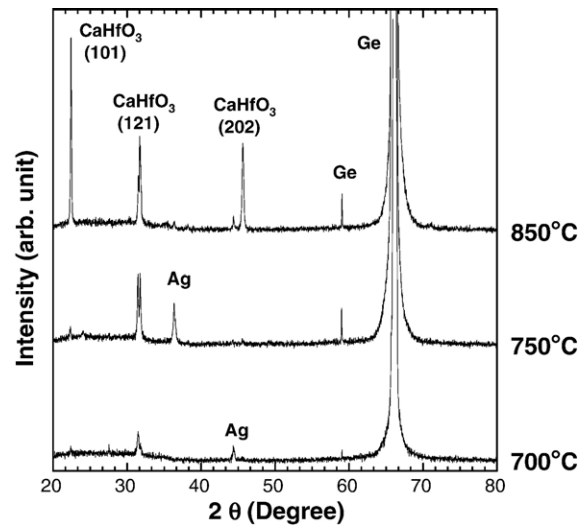

Fig. 6. X-ray diffraction scans of $CaHfO_3$ films on (001) Ge grown in vacuum at temperatures ranging from 500 to 700 °C.

pseudo-cubic $CaHfO_3$ (110) aligning with the Ni(001) surface normal. In-plane, there should be two domains (related by 90°), because $CaHfO_3$ (110) perp has only a two-fold symmetry while Ni(001) is four-fold. The sharper alignment is $CaHfO_3$ (001) aligned with the Ni (100); the broader alignment is $CaHfO_3$ (001) aligned with the Ni(010). The difference in peak widths and heights for these two domains indicates that the four-fold symmetry of the (001) Ni substrate has been broken. One possibility is that the rolling-induced scratches in the substrate lead to some degree of graphoepitaxy, which may also explain why the usual pseudo-cubic (001)-perp perovskite film orientation is not observed.

In order to further assess the growth behavior of $CaHfO_3$ on non-oxide substrates, the growth of $CaHfO_3$ on Ge(001) was also examined. The development of crystallographic texture with growth temperature was similar to that observed for growth on Ni. Fig. 6 shows the crystallinity of $CaHfO_3$ thin films grown at the temperatures from 700 to 850 °C at vacuum with the repetition rate of 2 Hz. In particular, at 750 °C, the dominant peaks correspond to the $CaHfO_3$ (121) orientation. This corresponds to the (110) pseudo-cubic perovskite orientation as seen for growth on Ni at low temperature. Increasing the growth temperature to 850 °C results in the emergence of (101) and (202) peaks, corresponding to the pseudo-cubic (001) orientation. Note that textured (101) growth was not observed for films grown on Si substrates. The major difference between Si and Ge substrates is the stability of the amorphous native oxide on Si at the growth temperature. The texture in the $CaHfO_3$/Ge case is assumed to originate from local epitaxy of $CaHfO_3$ with the Ge substrate. Deposition of $CaHfO_3$ on Si resulted in random orientation.

In conclusion, the growth behavior of $CaHfO_3$ on non-oxide substrates was examined. The tendency for $CaHfO_3$ growth at lower temperatures on both (001) Ni and (001) Ge substrates is to orient with the $CaHfO_3$ (200)+(121) peaks perpendicular, which corresponds to the (110) orientation in the pseudo-cubic geometry. At higher temperatures, the pseudo-cubic (001) orientation also appears.

Acknowledgements

This work was partially supported by the Army Research Office through research grant DAAD 19-01-1-0508 grant. The

authors would also like to acknowledge the staff of the Major Analytical Instrumentation Center, Department of Materials Science and Engineering, University of Florida, for their assistance with this work. ORNL research sponsored by the Division of Materials Science, US Department of Energy, under contract with UT-Battelle, LLC.

References

[1] Z. Yu, Y. Liang, H. Hi, J. Curless, C. Overgaard, R. Droopad, Y. Wei, X. Hu, B. Craigo, et al., Crystalline Oxide–Silicon Heterostructures and Oxide Optoelectronics, Symposium (Mater. Res. Soc. Symposium Proceedings), vol. 747, 2003, pp. 31–42.
[2] I. Bozovic, J.N. Eckstein, MRS Bulletin 20 (32) (1995).
[3] J.C. Jiang, X.Q. Pan, W. Tian, C.D. Theis, D.G. Schlom, Applied Physics Letters 74 (1999) 2851.
[4] D.H.A. Blank, G.J.H.M. Rijnders, G. Koster, H. Rogalla, Journal of Electroceramics 4 (2000) 311.
[5] I. Ohkubo, H.M. Christen, P. Khalifah, S. Sathyamurthy, H.Y. Zhai, C.M. Rouleau, D.G. Mandrus, D.H. Lowndes, Applied Surface Science 223 (2004) 35.
[6] J.Q. He, C.L. Jia, V. Vaithyanathan, D.G. Schlom, J. Schubert, A. Gerber, H.H. Kohlstedt, R.H. Wang, Journal of Applied Physics 97 (2005) 104921.
[7] R.A. McKee, F.J. Walker, M.F. Chisholm, Physical Review Letters 81 (1998) 3014.
[8] J.W. Reiner, F.J. Walker, R.A. McKee, C.A. Billman, J. Junquera, K.M. Rabe, C.H. Ahn, Physica Status Solidi. B, Basic Research 241 (2004) 2287.
[9] K. Shibuya, T. Ohnishi, T. Uozumi, M. Lippmaa, H. Koinuma, Thin Solid Films 486 (2005) 195.
[10] A. Goyal, D.P. Norton, Budai, M. Paranthaman, E.D. Specht, D.M. Kroeger, D.K. Christen, Q. He, B. Saffian, F. List, et al., Applied Physics Letters 69 (1996) 1795.
[11] D.P. Norton, A. Goyal, J.D. Budai, D.K. Christen, D.M. Kroeger, E.D. Specht, Q. He, B. Saffian, M. Paranthaman, C. Klabunde, et al., Science 274 (1996) 755.
[12] G. Fabricius, Y. Peltzer, E.L.P. Blanca, C.O. Rodriguez, A.P. Ayala, P. De la Presa, A.L. Garcia, Physical Review B 55 (1997) 164.
[13] G.B. Senft, V.S. Stubican, Materials Research Bulletin 18 (1983) 1163.
[14] J.L. Zhang, J.E. Evetts, Journal of Materials Science 29 (1994) 778.
[15] H. Yamamoto, M. Mikami, Y. Shimomura, Y. Oguri, Journal of Luminescence 87–89 (2000) 1079.
[16] Y.M. Ji, D.Y. Jiang, Z.H. Wu, T. Feng, J.L. Shi, Materials Research Bulletin 40 (2005) 1521.
[17] K. Shibuya, T. Ohnishi, M. Lippmaa, M. Kawasaki, H. Koinuma, Applied Physics Letters 84 (2004) 2142.
[18] Y.W. Kwon, D.P. Norton, G.E. Jellison Jr., Solid-State Electronics 47 (2003) 2149.